

See discussions, stats, and author profiles for this publication at: <https://www.researchgate.net/publication/261137205>

# Ambient Mass Spectrometry Imaging: Plasma Assisted Laser Desorption Ionization Mass Spectrometry Imaging and Its Applications

ARTICLE in ANALYTICAL CHEMISTRY · MARCH 2014

Impact Factor: 5.64 · DOI: 10.1021/ac403310k · Source: PubMed

---

CITATIONS

2

READS

61

## 10 AUTHORS, INCLUDING:



Jialing Zhang

3M

17 PUBLICATIONS 177 CITATIONS

[SEE PROFILE](#)



Min Li

13 PUBLICATIONS 110 CITATIONS

[SEE PROFILE](#)



Yu Bai

Peking University

74 PUBLICATIONS 869 CITATIONS

[SEE PROFILE](#)



Huwei Liu

Peking University

192 PUBLICATIONS 2,633 CITATIONS

[SEE PROFILE](#)

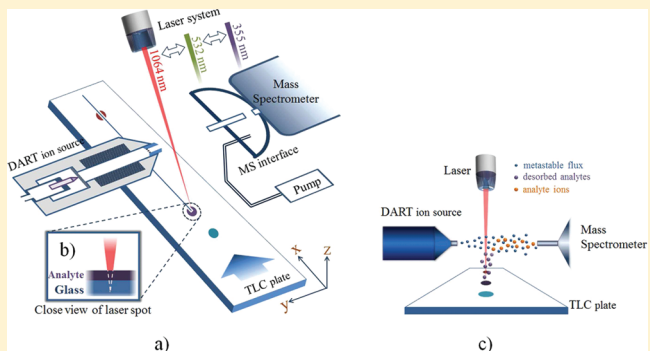
# Thin Layer Chromatography/Plasma Assisted Multiwavelength Laser Desorption Ionization Mass Spectrometry for Facile Separation and Selective Identification of Low Molecular Weight Compounds

Jialing Zhang, Zhigui Zhou, Jianwang Yang, Wei Zhang, Yu Bai,\* and Huwei Liu

Beijing National Laboratory for Molecular Sciences, Key Laboratory of Bioorganic Chemistry and Molecular Engineering of Ministry of Education, Institute of Analytical Chemistry, College of Chemistry and Molecular Engineering, Peking University, Beijing, 100871, P. R. China

## Supporting Information

**ABSTRACT:** A novel plasma assisted multiwavelength (1064, 532, and 355 nm) laser desorption ionization mass spectrometry (PAMLDI-MS) system was fabricated and applied in the analysis of low molecular weight compounds through combination with thin layer chromatography (TLC). The TLC/PAMLDI-MS system successfully integrated TLC, the multiwavelength laser ablation, and the excited state plasma from direct analysis in real time (DART) and was proved to be effective in the facile separation and selective identification of low molecular weight compounds. An automated three-dimensional platform was utilized to facilitate the analysis procedures with all the parameters of the TLC/PAMLDI-MS systematically optimized, and the desorption/ionization mechanisms were discussed. The successful combination of three-wavelength laser with DART based system extended the range of the analytes and provided broad possibilities for the compound desorption from the TLC. The experimental results clearly showed that the laser desorption was wavelength dependent. The PAMLDI-MS system was successfully applied in the detection of low molecular weight compounds from different kinds of samples separated on a normal-phase silica gel, such as dye mixtures, drug standards, and tea extract, with the detection level of 5 ng/mm<sup>2</sup>.



Owing to its attractive features such as high sample throughput, accessibility for postchromatographic evaluation, and requirement for minimal sample cleanup, thin layer chromatography (TLC) has been considered as a rapid, robust, and cost-effective method for mixture separation.<sup>1,2</sup> It has been used for large scale surveillance programs,<sup>3,4</sup> class fractionation and species separation of lipids,<sup>5,6</sup> and the analysis of complex and “dirty” samples.<sup>7</sup> In recent years, TLC makes continuous progress with the development of two-dimensional (2D) TLC<sup>8,9</sup> and the introduction of new techniques like pneumatic or electroosmotically driven flow TLC.<sup>10</sup>

MS offers high sensitivity, high specificity, and structural information for the unknowns,<sup>11,12</sup> which make it a preferred technique in the combination with TLC. The coupling of TLC and MS technique dates back to the late 1960s and has been of great interest ever since. Matrix-assisted laser desorption/ionization (MALDI) is a very popular ionization approach utilized for their coupling.<sup>13–15</sup> Other mass spectrometric methods, like fast atom bombardment mass spectrometry (FAB-MS),<sup>16</sup> plasma desorption,<sup>17</sup> and surface assisted laser desorption/ionization (SALDI)<sup>18</sup> MS have been utilized to analyze compounds separated by TLC. Nevertheless, the requirement of a high vacuum for these ion sources results in the postseparation preparation of the plates prior to analysis

and the need of specialized plates, and the interferences from the MALDI matrix have limited the applications of these techniques.

Ambient mass spectrometry,<sup>19</sup> which is operated in atmospheric environment and requires minimal sample preparation, provides a powerful analytical tool to substantially expand the scope of techniques which can be coupled to TLC. The two most popular ambient ionization techniques, desorption electrospray ionization (DESI)<sup>20</sup> and direct analysis in real time (DART),<sup>21</sup> have already been used in combination with TLC in 2005<sup>22</sup> and 2007,<sup>23</sup> respectively. After the introduction of DESI and DART, other ambient ion sources, such as atmospheric pressure chemical ionization (APCI),<sup>24</sup> desorption atmospheric pressure photoionization (DAPPI),<sup>25</sup> easy ambient sonic spray ionization (EASI),<sup>26,27</sup> dielectric barrier discharge ionization (DBDI),<sup>28</sup> laser ablation electrospray ionization (LAESI),<sup>29</sup> extractive electrospray ionization (EESI),<sup>30</sup> electrospray-assisted laser desorption ionization (ELDI),<sup>31</sup> low temperature plasma (LTP) probe,<sup>32</sup> laser induced acoustic desorption/electrospray ionization (LIAD/

Received: October 15, 2011

Accepted: December 15, 2011

Published: December 15, 2011



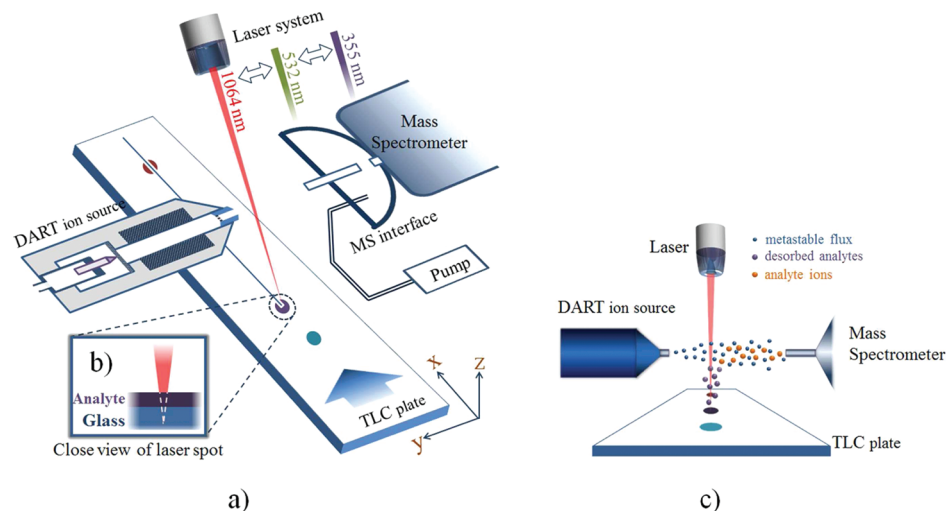


**Figure 1.** (a) Schematic illustration of the TLC/PAMLDI-MS setup. (b) Inset displaying close view of the relative position of the laser focal point and the plane of the TLC surface. (c) Proposed desorption and ionization processes of the TLC/PAMLDI-MS.

ESI),<sup>33,34</sup> and laser ablation metastable-induced chemical ionization (LAMICI)<sup>35</sup> are reported in succession. Among these innovations, ion sources with laser desorption or ablation have shown their “shining points” in spatial resolution when they are coupled to TLC. It is much more interesting to see the differences between compounds when the infrared (IR), visible, and ultraviolet (UV) laser are integrated in the ion source as the desorption approach after TLC separation.

In this study, a plasma-based ionization technique coupled with a multiwavelength laser system called PAMLDI has been fabricated and employed to characterize different analytes separated on TLC plates. Systematic optimization of the parameters of TLC/PAMLDI-MS was performed. Compared with other ambient ion sources, the three-wavelength laser (IR, visible, and UV) provided multiple choices for the detection of different compounds according to their specific absorptive wavelengths. The newly developed TLC/PAMLDI mass spectrometric method shows vigorous capability to detect many kinds of low molecular weight compounds.

## EXPERIMENTAL SECTION

**Chemicals and Reagents.** Rhodamine B, fluorescein, Sudan III, and methyl violet were obtained from Beijing Chemical Works (Beijing, China). Chloramphenicol, nateglinide, and gliclazide were purchased from the National Institute for the Control of Pharmaceutical and Biological Products (Beijing, China). Quinine was purchased from Alfa Aesar (Ward Hill, MA). A longjing tea sample was purchased from the local market in China. Methanol of HPLC grade and purified water were obtained from Dikma Technologies Inc. (California) and Hangzhou Wahaha Group Co., Ltd. (Zhejiang, China), respectively. Cellulose-coated TLC glass sheets (thickness, 0.25 mm, with fluorescent indicator, G/UV 254) and silica gel-coated TLC glass sheets (thickness, 0.2 mm, with fluorescent indicator, G/UV 254) were purchased from Anhui Liangchen Silicon Material Co., Ltd. (Anhui, China) and Kangbinuo Chemical Reagent Factory (Shandong, China), respectively.

**Fabrication of TLC/PAMLDI-MS System.** Figure 1a shows a schematic illustration of the ambient TLC/PAMLDI-MS experimental setup. The mass spectrometer used was Agilent XCT ion trap (Agilent Technologies, Palo Alto, CA)

equipped with a DART ion source (IonSense, Inc., Saugus, MA). A membrane pump (Vacuubrand, Wertheim, Germany), connected to the interface chamber, was utilized to remove the excess discharge gas flowing into the mass spectrometer inlet and balance the vacuum of the mass spectrometer. The Nd:YAG laser (Lai Yin Opto-Electronics Technology, Beijing, China) was chosen to provide three wavelengths laser (1064, 532, and 355 nm) with a pulse length of 10 ns at 10 Hz. The angle between the laser beam and TLC plate was kept as 45°. A three-dimensional autocontrol platform (STEP Motion Control System Engineering Co., Ltd., Shanghai, China) and a homemade TLC plate holder were used to exactly manipulate the position of the TLC plate. The 3D-platform can be operated remotely by either computer or the joystick (*x,y,z*) integrated into the control unit.

The mass spectrometric parameters in the positive ion mode were listed as follows: capillary voltage -3500 V, end plate offset -500 V, dry gas temperature 325 °C, and dry gas flow rate 5 L/min. The full-scan was carried out at the range of *m/z* 50–800 with a maximum ion accumulation time of 200 ms. The LC/MSD Trap Data Analysis (Agilent in-house version) was utilized to analyze the obtained data.

The working gas of the DART ion source was helium at 2.3 L/min, which was controlled by a flow meter (Flow Meter Factory, Yuyao, Zhejiang, China). The potential on the discharge needle electrode was set to 6000 V and the grid voltage was at 350 V.

**Standard Solutions.** The concentrations of dye mixtures in the methanol were 6.3 mmol/L for rhodamine B, 6.0 mmol/L for fluorescein, and 8.5 mmol/L for Sudan III. Standard solutions of drugs were prepared for TLC separation by dissolving the compounds in methanol at the concentration of 9.3 mmol/L for quinine, 9.3 mmol/L for gliclazide, and 9.3 mmol/L for chloramphenicol. Solution standards used for optimization of TLC/PAMLDI-MS were all prepared at a concentration of 6 mg/mL.

**Preparation of Longjing Tea Sample.** In total, 1 g of ground Longjing tea leaves was ultrasonically extracted for 20 min with 10 mL of methanol/H<sub>2</sub>O (70/30, v/v). Then, the extract was filtered, concentrated, and developed by normal phase silica gel-coated TLC.

**TLC Separation.** Both dye and drug standards mixtures were separated by normal phase silica gel-coated TLC plates. For the separation of dyes, the developing agent was dichloromethane/ethanol/ammonia (66.1:33.1:0.8, v/v/v). For the separation of drugs, the developing agent was hexane/ethanol/formic acid (64.7:32.4:2.9, v/v/v). For the tea extract, hexane/ethanol (1:2, v/v) was used as the developing agent. Samples and standards were spotted on the TLC sheet manually with a sampling capillary ( $\sim 1.0 \mu\text{L}/\text{sample}$ ). Developed plates were dried just by a hair dryer prior to analysis. In the case of the dyes, photographs of the developed plates were taken with a Panasonic FP1 digital camera (Panasonic Matsushita Electric Corporation of America, Secaucus, NJ) using white light illumination. A short wavelength (254 nm) UV lamp was used to determine the spot positions of drugs and tea extract, and their corresponding photographs were taken with the Panasonic FP1 digital camera. An IX71 inverted microscope (Olympus Corporation, Tokyo, Japan) was used to record the widths of the lanes of the fluorescein spotted TLC plates.

## RESULTS AND DISCUSSION

In recent years, ambient mass spectrometry has become a popular technique because of its great advantages in simplifying sample preparation steps and enhancing efficiency of the analysis. As a desorption tool, the laser possesses great ability in high-spatial resolution of analysis and holds great potential for mass spectrometry imaging. Therefore, it is hardly surprising that ambient mass spectrometric methods, coupled with laser techniques, have been reported continuously. For example, both ELDI<sup>31</sup> and LIAD/ESI<sup>34</sup> were used for characterizing organic compounds which were separated on TLC plates. Different wavelengths of lasers, such as IR, visible, and UV, can be used in this kind of coupling technique. However, the possibility that different laser might offer different desorption/ionization efficiency has seldomly studied. As discussed above, TLC coupling with an ambient ion source which contains a multiwavelength laser system must provide some original benefits. In the text below, the design, the optimum conditions of this new coupling technique, and its applications will be illustrated.

### Parameter Optimization of TLC/PAMLDI-MS System.

This new system was composed of TLC, a plasma-based ion generation technique, DART ion source, a multiwavelength laser system, and a mass spectrometer. Therefore, a systematic optimization will be necessary to acquire a satisfying MS response. Optimization of the signal levels of analytes was accomplished by detecting analytes spotted on several-centimeter long cellulose-coated TLC plates. The scanning speed was 0.1 mm/s. This method provided a relatively stable signal of the analytes for approximate 1–2 min during the optimization of one single parameter.

Although the temperature of plasma was an important factor for the DART ionization process,<sup>36</sup> it was not that much of a concern in the initial stage of our experiments. To obtain good MS signal, the gas flow rate was optimized to 2.3 L/min (data not shown). During the experiments, it was very interesting to find that heating of the plasma was still a necessary and key step during the whole experiment. We found that the higher the temperature, the better sensitivity it could achieve in PAMLDI-MS (Figure 2). In addition, for most of the compounds we selected, no target compounds were observed when the temperature was lower than 300 °C. This can be explained

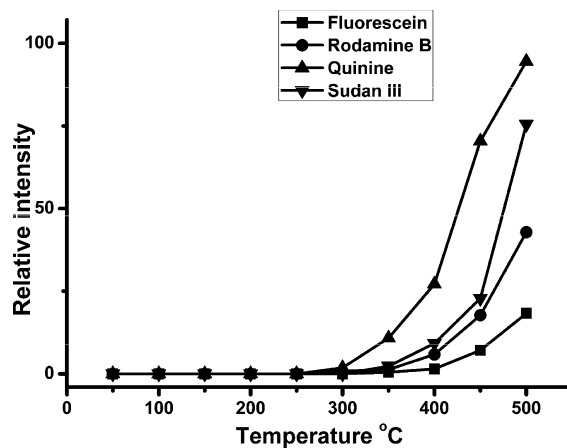
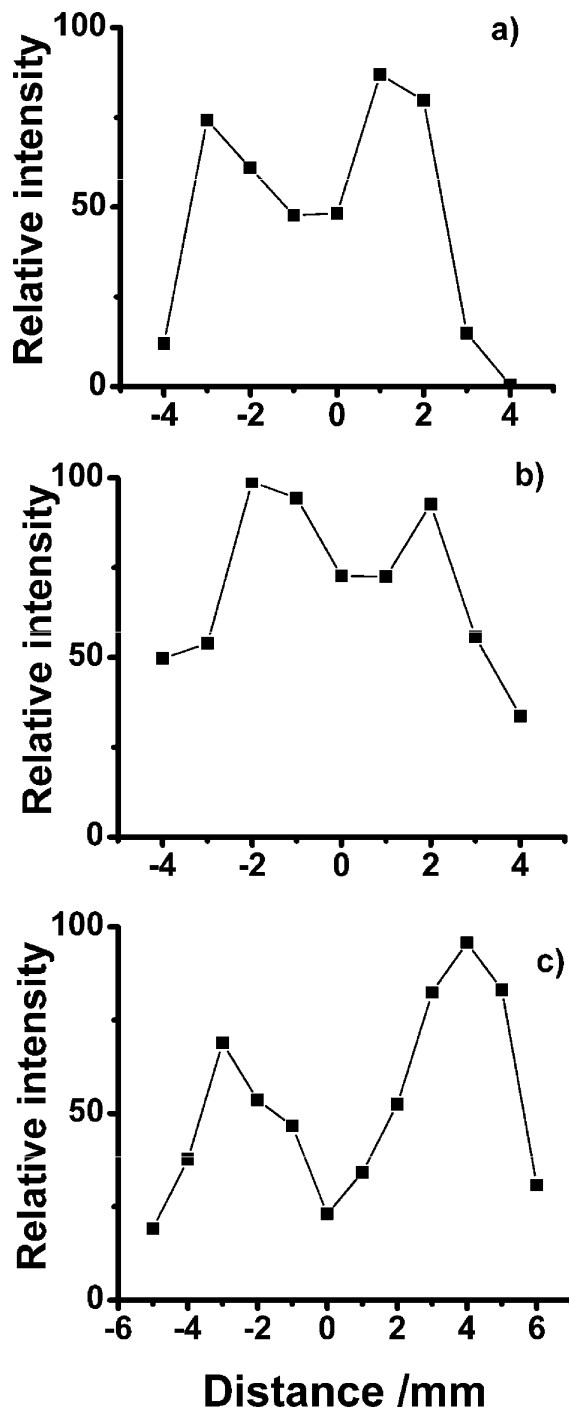


Figure 2. Optimization of the DART temperature for different compounds.

that higher temperature will enhance the internal energy (kinetic energy particularly) of metastable helium atoms, resulting in a better MS response. Considering the maintenance of the DART ion source, the temperature of 450 °C was selected for the detection of separated compounds on TLC plates.

As shown in Figure 1c, the metastable gas stream was in parallel with the TLC plate rather than aiming toward the TLC plate. The plasma produced in DART source reacted with the sample species desorbed from the TLC surfaces. A thermometer was utilized to test the temperature of the TLC surface. For each measurement, the thermometer was kept at the position for at least half an hour. The result showed that the surface temperature was only 45 °C, which was attributed to the low specific heat capacity of gas. Such a low temperature was not enough for the thermal desorption. In summary, no analytes ions from the TLC plate were observed when the laser was turned off. Therefore, we proposed that photodesorption dominates the desorption process of PAMLDI-MS.

During the optimization procedures, the relative distance between the focal point of the laser and the TLC plate and the laser energy were found to be two significant factors. Figure 3 shows the influence of the relative distance on the detection sensitivity. The distance “0” was defined as the position at which the focal point was focused right on the TLC plate, while “−” and “+” mean the distance of the focal point above and under the plate, respectively. Figure 1b provides a schematic view of the relation of the laser spot and the TLC plate, indicating the slightly off-center focal point was chosen to desorb the target compounds spotted on the TLC plate. For different laser wavelengths, 1064, 532, and 355 nm, the strongest signals were obtained in the position of 1–2, 2–3, and 3–4 mm, respectively. The signal generated by laser desorption right from the focal point was lower than that of the slightly off-center point, which might be attributed to two reasons: the sputtering of particles right in the focal point induced the decentralization of the desorbed neutral target species and led to the unstable signal and the decrease of the desorption area compared to that of the slightly off-center point. The optimization of the laser energy was conducted under the best focal position (data not shown). A bell-shaped curve was acquired when plotting signal intensity against laser energy. It can be explained that laser energy is not sufficient to desorb the target compounds when the laser energy was weak



**Figure 3.** Optimization of relative distance between the focal point of the laser and the TLC plate under different wavelengths of the laser: (a) 1064, (b) 532, and (c) 355 nm.

and, as discussed above, the sputtering effect will dominate the process when the laser energy was too strong. For acquiring strong and stable MS signals, the laser energy of different laser wavelengths, 1064, 532, and 355 nm, was set to 4.8–5.1, 1.8–2.0, and 1.0–1.2 mJ, respectively.

The influences of the distance between the DART exit and the ablation point, the distance between the ablation point and the ion transfer tube, and the height of the TLC plate and the plane of the DART exit and the ion transfer tube were also studied and set to 3, 13, and 3.5 mm, respectively.

**Characterization of Laser Lanes on TLC Plate.** Figure 4 shows the widths of lanes ablated by IR, visible, and UV lasers. It can be found that the narrowest lanes were provided by the UV laser among the three-wavelength lasers for both cellulose-coated plates and silica gel-coated plates. For cellulose-coated plates, approximately 220, 200, and 150  $\mu\text{m}$  lanes were generated by the IR, visible, and UV lasers, respectively. For silica gel-coated plates, approximately 400, 280, and 200  $\mu\text{m}$  lanes were generated by the IR, visible, and UV lasers, respectively. It has been confirmed that the spatial resolution of DART was approximate 3 mm.<sup>23</sup> Compared with the TLC/DART-MS, the TLC/PALDI-MS possesses greater potential for sampling and characterizing compounds within a small TLC spot.

**Wavelength Dependent Detection of Different Compounds.** In our TLC/PALDI-MS system, analyte desorption was completed by the laser. It can be predicted that the absorbance efficiency of the laser was varied for different kinds of compounds according to different laser wavelengths. The performance comparisons of different wavelength-laser were carried out with the best sensitivity of standards under each wavelength.

As shown in Figure 5, the strongest intensities were obtained under the visible wavelength (532 nm) for rhodamine B, Sudan III, and methyl violet. For quinine, chloramphenicol, gliclazide, and naglina, the best sensitivities were generated under the UV wavelength (355 nm). For the detection of fluorescein, we found that the UV and visible wavelengths of the laser provided better sensitivity than the IR wavelength (1064 nm). Since every molecule is capable of absorbing its own characteristic frequencies of electromagnetic radiation, this optical selectivity should be in accordance with the absorption law.

Molecules undergo three different types of quantized transitions, electronic transitions, vibration transitions, and rotational transitions, when excited by ultraviolet, visible, and infrared radiation. We have noted that the energy  $h\nu$  of the photon must be exactly the same as the energy difference between the two orbital energies. For quinine and chloramphenicol, the absorptive wavelengths caused by electronic transition of simple molecular lie in the region between 190 and 380 nm. It is noted that large conjugated systems which undergo a  $\pi$  to  $\pi^*$  transition tend to cause red shifts in the peak maxima to longer wavelengths. Therefore, absorption wavelengths of compounds like rhodamine B and Sudan III lie in the region between 380 and 750 nm. Therefore, quinine has a higher absorption efficiency under UV laser desorption than that under 532 or 1064 nm laser desorption. Likewise, the observation of a higher ion intensity while detecting rhodamine B using the visible laser can be explained.

The wavelength selectivity of this ambient ion source provides multiple choices for detecting different compounds. For example, when detecting an unknown compound, three wavelengths of the laser can be attempted successively to find the proper one for its desorption. Until now, we have not found the species showing a high tendency to be detected under the IR laser. Related work is still under study. However, Huang et al. reported that a stronger signal for the cytochrome c ion was observed when using an IR laser (1064 nm) for desorption, compared with that of the laser at wavelengths of 266 or 532 nm.<sup>37</sup> It was explained that the increase of the intensity was attributed to the absorption of near-IR radiation inducing OH bending vibrations of the  $\text{H}_2\text{O}$  molecules. We may benefit from

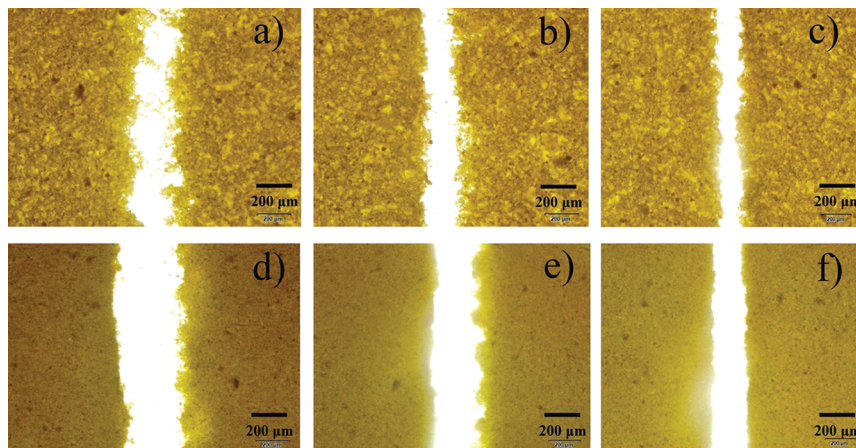


**Figure 4.** Photographs of ablated lanes of TLC plates with IR, visible, and UV lasers: (a) cellulose-coated TLC plate with IR laser, (b) cellulose-coated TLC plate with visible laser, (c) cellulose-coated TLC plate with UV laser, (d) silica gel-coated TLC plate with IR laser, (e) silica gel-coated TLC plate with visible laser, and (f) silica gel-coated TLC plate with UV laser.

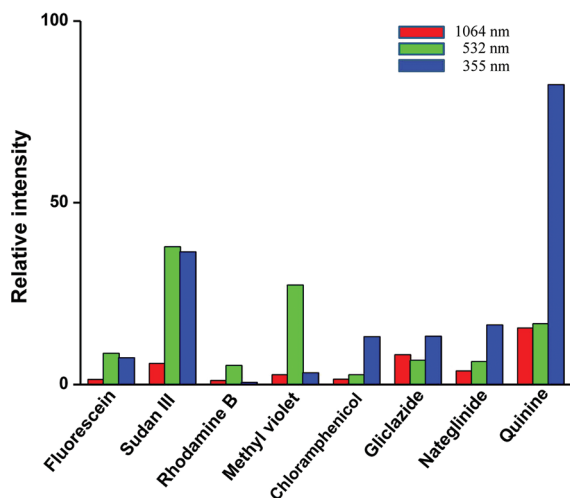


**Figure 5.** Variation of ion intensity of eight small molecules, which were desorbed by the Nd:YAG laser with a wavelengths of 355, 532, and 1064 nm, respectively.

this work to find compounds which can obtain the best sensitivity under the IR laser.

Another interesting phenomenon was observed when the spectra of rhodamine B under three wavelengths of laser were compared. All results were obtained under the optimized conditions in which laser energies of UV, visible, and IR were set to ~1, ~1.9, and ~5 mJ, respectively. Interestingly, although the absolute energy value of the UV laser is the lowest one, it was found that the highest relative abundance of fragment ions at  $m/z$  399 ( $[M - CO_2 + H]^+$ ) was obtained when the UV laser was used (see Figure 6). For the IR laser, the molecular ion of rhodamine B dominated in the mass spectrum. It has been testified that the photothermal process and the photochemical process govern the interaction between the laser and matter for the IR and UV lasers, respectively.<sup>38</sup> When a visible or IR wavelength of the laser was used, the dominant effect created in the desorption process was the thermal effect. So the laser serves as a heat source in this case. In another case, UV laser radiation encourages bond-breaking of analytes in a more severe extent, which is different from the IR and visible laser. As reported in the literature,<sup>44</sup> partial decomposition and fragmentation of the analytes might occur in the DART

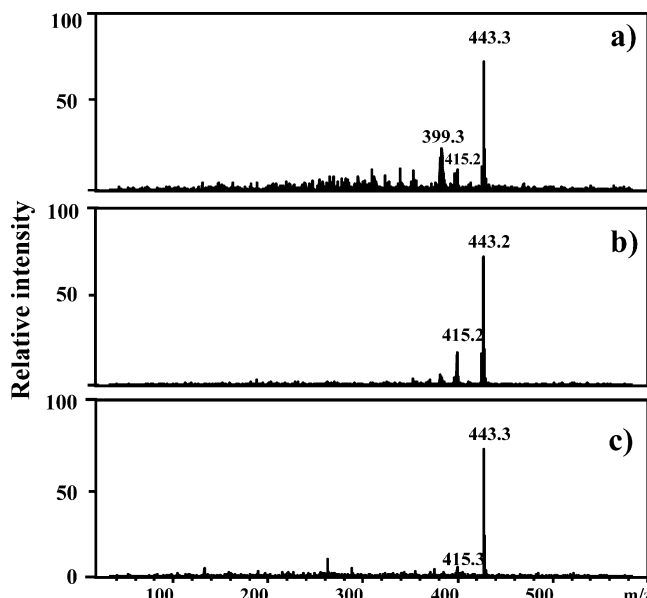


**Figure 6.** Mass spectra of rhodamine B under different wavelengths of the laser: (a) 355, (b) 532, and (c) 1064 nm.

ionization when the gas temperature is high enough. Target compounds have been analyzed by using DART-MS with the same parameters (see Figure S1 in the Supporting Information). When compared with those of DART-MS, more fragments were observed from the spectra of PAMLDI-MS. We hereby proposed that PAMLDI-MS induced more photodissociation than DART-MS during the ionization step.

**Application for the Real Sample Detection.** In this work, dyes, drugs, and tea leaf extracts were selected to test the performance of the PAMLDI-MS method. All separations were accomplished on normal phase silica gel-coated TLC plates. Figure 7 indicates that combining TLC with PAMLDI-MS allowed the detection of dyes and drugs separated on normal-phase TLC plates, in which protonated molecular ions were monitored during the experiments. As shown in Figure 1c, the assumed ionization processes were as follows: first, metastable helium atoms were produced via a corona-to-glow discharge transition;<sup>39</sup> when the laser-ablated gel particles crossed the metastable flux, the analyte molecules were rapidly released

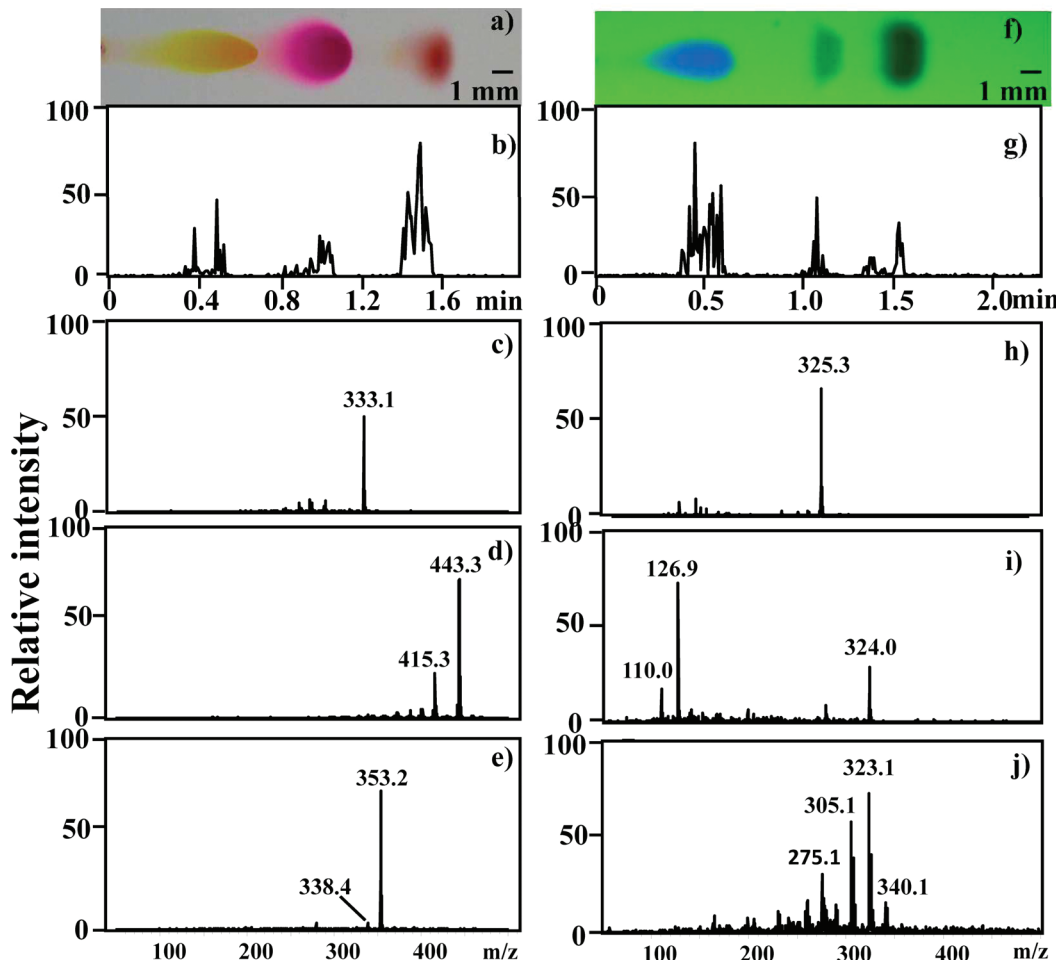


**Figure 7.** (a) Photograph of three separated dye standards on a silica gel-coated TLC plate. (b) Extracted ion chromatograms of fluorescein, rhodamine B, and Sudan III from left to right. Positive-ion TLC/PALDI mass spectra of (c) fluorescein, (d) rhodamine B, and (e) Sudan III. (f) Photograph of three separated drug standards on a silica gel-coated TLC plate. (g) Extracted ion chromatograms of quinine, gliclazide, and chloramphenicol from left to right. Positive TLC/PALDI mass spectra of (h) quinine, (i) gliclazide, and (j) chloramphenicol.

from the gel by the heat current and pried a proton from the water clusters which were generated by metastable helium atoms. Compared with other wavelengths, some fragments were generated through a photochemical process when the analytes were desorbed by the UV laser beam.

For the detection of dye standards (rhodamine B, Sudan III, and fluorescein), visible laser light (532 nm) was utilized. The photograph of a separated sample lane on the TLC plate was shown in Figure 7a. The values of  $R_f$  [(the migration distance of analyte)/(the migration distance of solvent front)] were 0.25, 0.52, and 0.75 for fluorescein, rhodamine B, and Sudan III, respectively. Figure 7b presents the extracted ion chromatograms of the fluorescein ( $m/z$  333), rhodamine B ( $m/z$  443), and Sudan III ( $m/z$  353). The positive PAMLDI mass spectra recorded at each spot of the dye standard mixture are displayed in Figure 7c–f. For the detection of rhodamine B, compared with the spectra obtained from DART-MS, fragment ions, such as  $[M - CO + H]^+$  ( $m/z$  415) and  $[M - CO_2 + H]^+$  ( $m/z$  399), were observed in visible-PAMLDI-MS. The MS/MS experiments of rhodamine B were carried out to confirm the results (data not shown). This feature of PAMLDI-MS has superiority in offering structure information of unknown compounds. In addition, the comparison of TLC/DART-MS with TLC/PAMLDI-MS (see Figure S2 in the Supporting Information) was made to prove the high spatial resolution

provided by PAMLDI-MS. All of the three dyes separated on the TLC plate and could be baseline resolved by PAMLDI-MS.

The separation of a mixture of drug standards (quinine, chloramphenicol, and gliclazide) were also performed using a UV lamp for the visualization of the sample spots ( $R_f$  of quinine, chloramphenicol, and gliclazide: 0.24, 0.50, and 0.64 respectively). After the position determination of each standard, the developed TLC plates were mounted onto the TLC plate holder and scanned by UV-PAMLDI-MS. Figure 7g shows the extracted ion chromatograms of quinine ( $m/z$  325), chloramphenicol ( $m/z$  323), and gliclazide ( $m/z$  324) in the positive mode. For the chloramphenicol, fragment ions at  $m/z$  305 and  $m/z$  275 were observed, which were attributed to the generation of  $[M - H_2O + H]^+$  and  $[M - H_2O - CH_2O + H]^+$ .<sup>40</sup> Two fragment ions of gliclazide came from the generation of  $[M - C_8H_8N_2O_3S + H]^+$  and  $[M - C_8H_8NO_3S + H]^+$ , which were consistent with our previous research.<sup>41</sup>

Finally, Chinese tea was selected to test the applicability of TLC/PAMLDI-MS for the analysis of a complex sample. Separation of the sample was fulfilled on a normal-phase silica gel-coated TLC plate, and the visualization of the TLC plate was carried out under a UV lamp (254 nm). Figure 8b–f displays the extracted ion chromatograms of five representative chemical compounds detected on the TLC plate ( $m/z$  131,

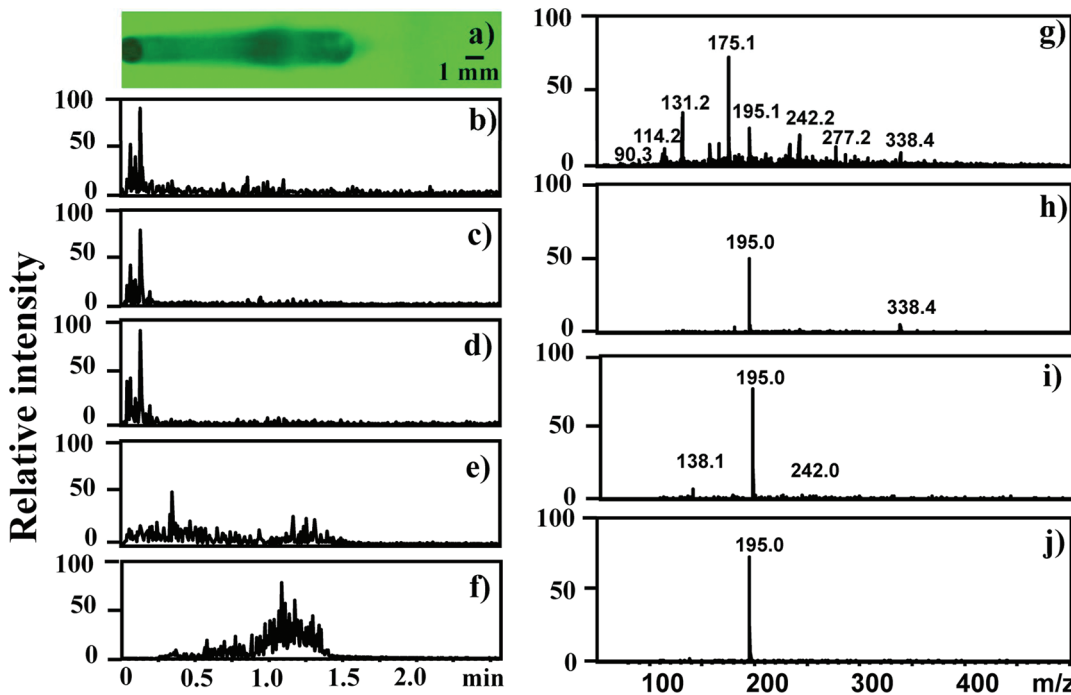


**Figure 8.** (a) Photograph of the separated components of the Chinese tea extract on a silica gel-coated TLC plate. Extracted ion chromatograms of the ions at  $m/z$  (b) 131, (c) 175, (d) 195, (e) 242, and (f) 338. Positive PAMLDI mass spectra recorded at  $R_f$  values of (g) 0.01, (h) 0.12, (i) 0.39, and (j) 0.44, respectively.

175, 195, 242, and 338) at various  $R_f$  values. Figure 8g–j presents positive mass spectra recorded from the spot with  $R_f$  values of 0.01, 0.12, 0.39, and 0.44, respectively. The peaks at  $m/z$  175 and 195 corresponded to theanine and caffeine.<sup>42,43</sup> Peaks at  $m/z$  138 in Figure 8i were attributed to the loss of the  $\text{CH}_3\text{NC}=\text{O}$  group from caffeine. In summary, TLC/PAMLDI-MS provided a rapid and successful screening approach for the detection of the complicated sample like Chinese tea extract.

## CONCLUSIONS

A new ambient ionization technique, plasma assisted multi-wavelength laser desorption ionization mass spectrometry (PAMLDI-MS), was successfully coupled with TLC for rapid analysis of complex samples. The three-wavelength laser system provides great advantages in detecting different species of low molecular weight compounds. Two kinds of standards, dye materials and drugs, were successfully developed by TLC and detected by using visible-PAMLDI-MS and UV-PAMLDI-MS, respectively. Detailed interpretations of the mass spectra obtained from IR, visible, and UV-PAMLDI-MS were discussed, which indicated that higher energy photons, like UV photons, resulted in a more severe extent of cleavage of bonds. The analysis of the extract of Chinese tea can also be successfully completed by the designed UV-PAMLDI-MS system. We are expecting a great application prospect of this ambient ion source, not only to couple with other novel techniques but also to be put into use in imaging mass spectrometry.

## ASSOCIATED CONTENT

### Supporting Information

Additional information as noted in text. This material is available free of charge via the Internet at <http://pubs.acs.org>.

## AUTHOR INFORMATION

### Corresponding Author

\*E-mail: [yu.bai@pku.edu.cn](mailto:yu.bai@pku.edu.cn). Phone: 86-10-62758198.

## ACKNOWLEDGMENTS

This work was financially supported by the National Natural Science Foundation of China (Grant Numbers 21027012, 20805001, and 21175008) and the fundamental research funds for the central universities.

## REFERENCES

- (1) Sherma, J. *Anal. Chem.* **2010**, *82*, 4895–4910.
- (2) Poole, C. F. *J. Chromatogr., A* **2003**, *1000*, 963–984.
- (3) Morlock, G. E. *J. Chromatogr., A* **1996**, *754*, 423–430.
- (4) Butz, S.; Stan, H. *J. Anal. Chem.* **1995**, *67*, 620–630.
- (5) Zellmer, S.; Lasch, J. *J. Chromatogr., B* **1997**, *691*, 321–329.
- (6) Muthing, J.; Ziehr, H. *J. Chromatogr., B* **1996**, *687*, 357–362.
- (7) Szepesi, G.; Nyiredy, S. *J. Pharm. Biomed. Anal.* **1992**, *10*, 1007–1015.
- (8) Han, Y. H.; Levkin, P.; Abarrientos, I.; Liu, H. W.; Svec, F.; Frechet, J. M. *J. Anal. Chem.* **2010**, *82*, 2520–2528.
- (9) Paglia, G.; Ifa, D. R.; Wu, C. P.; Corso, G.; Cooks, R. G. *Anal. Chem.* **2010**, *82*, 1744–1750.
- (10) Nyiredy, S. *J. Chromatogr., A* **2003**, *1000*, 985–999.
- (11) Cheng, S. C.; Huang, M. Z.; Shiea, J. *J. Chromatogr., A* **2011**, *1218*, 2700–2711.
- (12) Morlock, G.; Schwack, W. *TrAC, Trends Anal. Chem.* **2010**, *29*, 1157–1171.
- (13) Santos, L. S.; Haddad, R.; Hoehr, N. F.; Pilli, R. A.; Eberlin, M. N. *Anal. Chem.* **2004**, *76*, 2144–2147.
- (14) Gusev, A. I.; Proctor, A.; Rabinovich, Y. I.; Hercules, D. M. *Anal. Chem.* **1995**, *67*, 1805–1814.
- (15) Fuchs, B.; Schiller, J.; Suss, R.; Schurenberg, M.; Suckau, D. *Anal. Bioanal. Chem.* **2007**, *389*, 827–834.
- (16) Oka, H.; Ikai, Y.; Ohno, T.; Kawamura, N.; Hayakawa, J.; Harada, K.; Suzuki, M. *J. Chromatogr., A* **1994**, *674*, 301–307.

- (17) Danigel, H.; Schmidt, L.; Jungclas, H.; Pfluger, K. H. *Biomed. Mass Spectrom.* **1985**, *12*, S42–S44.
- (18) Chen, Y. C.; Shiea, J.; Sunner, J. *J. Chromatogr., A* **1998**, *826*, 77–86.
- (19) Cooks, R. G.; Ouyang, Z.; Takats, Z.; Wiseman, J. M. *Science* **2006**, *311*, 1566–1570.
- (20) Takats, Z.; Wiseman, J. M.; Gologan, B.; Cooks, R. G. *Science* **2004**, *306*, 471–473.
- (21) Cody, R. B.; Laramee, J. A.; Durst, H. D. *Anal. Chem.* **2005**, *77*, 2297–2302.
- (22) Van Berkel, G. J.; Ford, M. J.; Deibel, M. A. *Anal. Chem.* **2005**, *77*, 1207–1215.
- (23) Morlock, G.; Ueda, Y. *J. Chromatogr., A* **2007**, *1143*, 243–251.
- (24) Peng, S.; Ahlmann, N.; Kunze, K.; Nigge, W.; Edler, M.; Hoffmann, T.; Franzke, J. *Rapid Commun. Mass Spectrom.* **2004**, *18*, 1803–1808.
- (25) Haapala, M.; Pol, J.; Saarela, V.; Arvola, V.; Kotiaho, T.; Ketola, R. A.; Franssila, S.; Kauppila, T. J.; Kostiainen, R. *Anal. Chem.* **2007**, *79*, 7867–7872.
- (26) Eberlin, L. S.; Abdnur, P. V.; Passero, A.; de Sa, G. F.; Daroda, R. J.; de Souza, V.; Eberlin, M. N. *Analyst* **2009**, *134*, 1652–1657.
- (27) Haddad, R.; Milagre, H. M. S.; Catharino, R. R.; Eberlin, M. N. *Anal. Chem.* **2008**, *80*, 2744–2750.
- (28) Na, N.; Zhao, M. X.; Zhang, S. C.; Yang, C. D.; Zhang, X. R. *J. Am. Soc. Mass Spectrom.* **2007**, *18*, 1859–1862.
- (29) Nemes, P.; Vertes, A. *Anal. Chem.* **2007**, *79*, 8098–8106.
- (30) Chen, H. W.; Venter, A.; Cooks, R. G. *Chem. Commun.* **2006**, 2042–2044.
- (31) Lin, S. Y.; Huang, M. Z.; Chang, H. C.; Shiea, J. *Anal. Chem.* **2007**, *79*, 8789–8795.
- (32) Harper, J. D.; Charipar, N. A.; Mulligan, C. C.; Zhang, X. R.; Cooks, R. G.; Ouyang, Z. *Anal. Chem.* **2008**, *80*, 9097–9104.
- (33) Cheng, S. C.; Cheng, T. L.; Chang, H. C.; Shiea, J. *Anal. Chem.* **2009**, *81*, 868–874.
- (34) Cheng, S. C.; Huang, M. Z.; Shiea, J. *Anal. Chem.* **2009**, *81*, 9274–9281.
- (35) Galhena, A. S.; Harris, G. A.; Nyadong, L.; Murray, K. K.; Fernandez, F. M. *Anal. Chem.* **2010**, *82*, 2178–2181.
- (36) Cody, R. B. *Anal. Chem.* **2009**, *81*, 1101–1107.
- (37) Huang, M. Z.; Jhang, S. S.; Cheng, C. N.; Cheng, S. C.; Shiea, J. *Analyst* **2010**, *135*, 759–766.
- (38) Lafargue, P. E.; Chaoui, N.; Millon, E.; Muller, J. F.; Deruelle, H.; Popadenec, A. *Surf. Coat. Technol.* **1998**, *106*, 268–276.
- (39) Shelley, J. T.; Hieftje, G. M. *J. Anal. At. Spectrom.* **2010**, *25*, 345–350.
- (40) Hammel, Y. A.; Mohamed, R.; Gremaud, E.; LeBreton, M. H.; Guy, P. A. *J. Chromatogr., A* **2008**, *1177*, 58–76.
- (41) Zhou, Z. G.; Zhang, J. L.; Zhang, W.; Bai, Y.; Liu, H. W. *Analyst* **2011**, *136*, 2613–2618.
- (42) Ford, M. J.; Deibel, M. A.; Tomkins, B. A.; Van Berkel, G. J. *Anal. Chem.* **2005**, *77*, 4385–4389.
- (43) Zhu, X. L.; Chen, B.; Ma, M.; Luo, X. B.; Zhang, F.; Yao, S. Z.; Wan, Z. T.; Yang, D. J.; Hang, H. W. *J. Pharm. Biomed. Anal.* **2004**, *34*, 695–704.
- (44) Chernetsova, E. S.; Morlock, G. E.; Revelsky, I. A. *Russ. Chem. Rev.* **2011**, *80*, 235–255.